22nd IAHR International Symposium on Ice
Singapore, August 11 to 15, 2014

Texture-based sea ice classification on TerraSAR-X imagery

Rudolf Ressel, Susanne Lehner
German Center for Air and Space Research DLR, IMF
Henrich Focke Str. 4, 28199 Bremen, Germany
rudolf.ressel@dlr.de

Sea ice monitoring has attracted growing attention over the last decade due to its importance in global warming. Besides the purely scientific interest, practical implications of global warming are the increased navigability of ice-infested sea passages such as the Arctic Northwestern and Northeastern passages. To assist maritime endeavors in these areas, ice type classification is pivotal. National sea ice surveillance services of several countries have provided ice charts on a continuous basis, mostly generated by human experts in a manual fashion. These classifications are based on a variety of data sources, mostly from microwave or optical spaceborne and airborne sources. In this paper we present an approach that relies on TerraSAR-X Satellite data. Such data offers images at a high resolution in a radar band so far very rarely applied for ice classification. In order to build on expert knowledge of the past, we designed an artificial neural network approach, which outputs a number of suitable ice type classes. Input neurons are fed by an automated feature extraction algorithm. These features are based on popular and well-established texture analysis methods, most notably graylevel co-occurrence matrices (GLCM) and local binary patterns (LBP). Images are acquired for a selected geographical area for which ground truth data can be obtained from national ice services (Baltic sea). From these datasets, training and validation samples are chosen and evaluated. Classification results are compared with official ice charts. We asses suitability for near real time services. Based on first examples and computed results, we conclude that our approach is rather promising for automatic near real time (NRT) services.

Proceedings of the 22nd IAHR International Symposium on Ice

ISBN: 978-981-09-0750-1
doi:10.3850/978-981-09-0750-1_1243

1. Introduction

Spaceborne SAR surveillance of ice-infested Arctic waters is comparably independent of lighting and cloud coverage conditions. In contrast to airborne and shipborne SAR, spaceborne SAR can acquire images over otherwise inaccessible regions without long waiting times and at high recurring frequencies. These qualities have popularized the use of satellite SAR for such research topics as ice and iceberg drift, sea state in ice and ice type classification. The latter topic will be the focus of this work. Similar studies in the past on ice type identification in SAR images (Soh 1999, Soh 2004, Bogdanov 2005, Zakhvatkina 2012, Clausi 2010, Dierking 2012, Karvonen 2004) discussed mostly C-band data. In our analysis, we use high resolution data in X-band provided by the TerraSAR-X satellite. To the authors' knowledge, very little research has been conducted on TerraSAR-X data for sea ice classification so far (cf. Moen 2013). We therefore further investigate the usefulness of TerraSAR-X data for ice type classification for a particular geographic region (Baltic Sea) dating from winter/spring 2014. Since the goal of our work is to automatically generate ice charts for operational use, only ScanSAR images are employed. In the case of TerraSAR-X, ScanSAR images are delivered only as single pol data. Therefore, polarimetric tools cannot be applied on these datasets, but only classical image analysis. Since a pixel based analysis is insufficient for separating different ice classes, we resort to well-established texture based methods. Among these are gray level co-occurrence matrices (GLCM) (cf. Bogdanov 2005, Zakhvatkina 2012, Soh 1999, Clausi 2010 and references therein), autocorrelation methods (Karvonen 2004), wavelet based features (Yu 2002), Gabor wavelet techniques (Clausi 2010), and MRF (Clausi 2010). Due to their reported suitability (Bogdanov 2005, Clausi 2010), we have chosen to conduct our texture analysis in this work with GLCM features. These techniques assign a vector of numerical features to small neighborhoods of the image. A supervised classifier then assigns an output ice type to such a feature vector. For the problem of picking training data, we rely on our own visual judgement, official ice charts of national ice services and experience with SAR imagery of sea ice. For the classifier, artificial neural networks have been used successfully on ice classification problems, for which reason we employ an open source neural network library (FANN) for our purposes.

2. Methods

Texture feature extraction is commonly carried out by sliding a window of fixed size (eg. 11x11, 31x31 pixels) over the entire image with an shift offset of 1,2,3,... pixels for the sliding window. The sliding window represents the neighborhood of the center pixel and all arithmetic or statistical computations are performed on this neighborhood. The extracted features are then attributed to the center pixel as a qualifier for the texture surrounding the center pixel.

For GLCM, one first picks a parameter for the sliding window size. On this window (after rebinning grayvalues to eg. 64 graylevels) one then computes the histogram of neighboring pixel pairs of two pixels, with a fixed interpixel distance of the two pixels and fixed orientation of the pair axis. The resulting histogram in geometric order is the so-called graylevel co-occurrence matrix (GLCM). We chose 11x11 sliding windows for the analysis. Windowsizes 31x31 and 65x65 were computationally more expensive and exhibited a stronger block effect on the ice charts. We then fixed the interpixel distance to one pixel, and computed the GLCM for the pair axis with orientations west, northwest, north and northeast. The matrices for the four directions (west, northwest, north and northeast) are then summed to arrive at one resulting matrix. Only on this combined histogram we compute the five common GLCM features entropy, uniformity, contrast, homogeneity, energy (see formulae in Clausi 2010, Haralick 1973) and five moment features (first-fourth moment, log moment). Additional measures commonly used can be found in (Clausi 2010, Haralick 1973).

To generate LBP features (Ojala 1994) for one pixel of an image, one takes a circular neighborhood of pixels, eg. the eight immediate neighbor pixels of the center pixel. Then one compares the center pixel and each of mentioned neighbor pixels in clockwise order. When the center pixel's gray value is larger than that of the neighboring pixel, the comparison yields 1, otherwise 0. By this procedure, each pixel of an image (except for marginal pixels) is assigned a binary pattern of eight pixels (or more pixels depending on the length of the circular neighborhood). This binary pattern encodes the sign of the local gray value gradient, serving as a texture feature. To reduce the number of possible features, one commonly identifies rotationally invariant features. To reduce the number of features further, all features with more than two 0-1 transitions are fused into one feature, called non-uniform features (Mäenpää 2000). One thus ends up with 8 uniform binary patterns and one non-uniform LBP.

The relevant features for ice classification occur on a larger scale. Therefore, it is most suitable to downscale the image size before extracting features. Besides matching the texture extraction to the texture scale of the image, one also avoids considerable computational overhead (which must be kept in mind for NRT processing). To avoid the beam-banding related texture artifacts, we work on a reduced image scale and on the single strips that compose the full ScanSAR image.

Calibration was performed to arrive at σ_0 values (not in dB scale) according the official technical documentation of TerraSAR-X data. All feature extraction was performed on these σ_0 values.

3. Classification

For the classification algorithm we used a well-established open source code of a neural network library in C (FANN, cf. Nissen 2005). The input had 19 input neurons. The first hidden layer had eight hidden neurons and the second hidden layer had nine hidden neurons. For the output we had four output neurons for each of the ice types.

Before feeding the feature vectors into the neural network one needs to rescale the vectors into the range of (-1,1) since the propagation functions are commonly only defined on the domain (-1,1) or a similarly compact interval. In order to mitigate the effect of outliers we use the following tanh rescaling:

$$z_i = \tanh\left(\frac{x_i - \mu_i}{\sigma_i}\right) \quad \textbf{[1]}$$

where x_i denotes one entry of a feature vector, μ_i denotes the mean of i-th entries of all feature vectors of the image, and σ_i denotes the standard deviation of the i-th entries of all feature vectors of the image. This mitigates the effect of outliers and scales. Besides the domain requirements of the classifier, the normalization in the argument of the tanh function is further justified by the following statistical considerations: Since the features should have the same statistical behavior in different images, normalizing each feature vectors with the respective global mean and standard deviation would lead to the same statistical clustering properties of the different ice types.

The training comprised less than 0.2% of the entire image in terms of pixels.

4. Results

As test dataset we use a WideScanSAR image of the Northern Baltic Sea (Bottenvik) off the Eastern Svalbard coast. The images for the Bottenvik were acquired on Feb, 27, 2014.

WideScansar Northern Baltic Sea, Feb, 27, 2014

The choice of predominant ice types proved to be a rather delicate task. By the guidance of an ice expert and visual inspection, we arrived at an ice type array of four different ice types: open water, smooth ice (comprising mostly fast ice and smooth fast ice floes), moderately deformed pack ice (which includes most parts of the pack ice zone), and highly deformed ice types (including ridges, hummocks, brash barriers). Multiyear ice does not occur in the Baltic Sea.

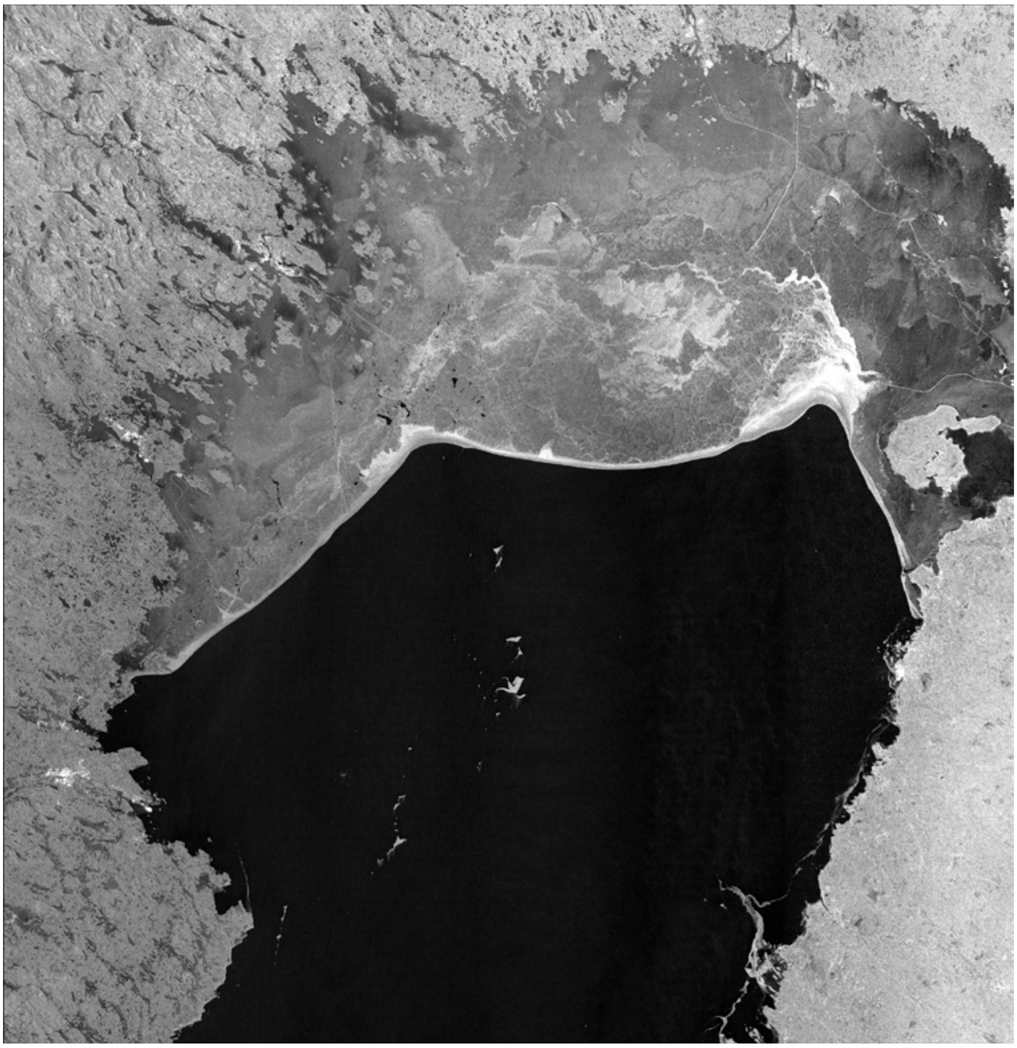

Figure 1. TerraSAR-X WideScanSAR image Feb, 27, 2014

Blue indicates open water, bright green is highly deformed pack ice (including ridges, brash windrows, hummocked ice), medium green is moderately deformed ice (includes portions of fast ice), dark green indicates smooth ice (mostly fast ice and fast ice floes).

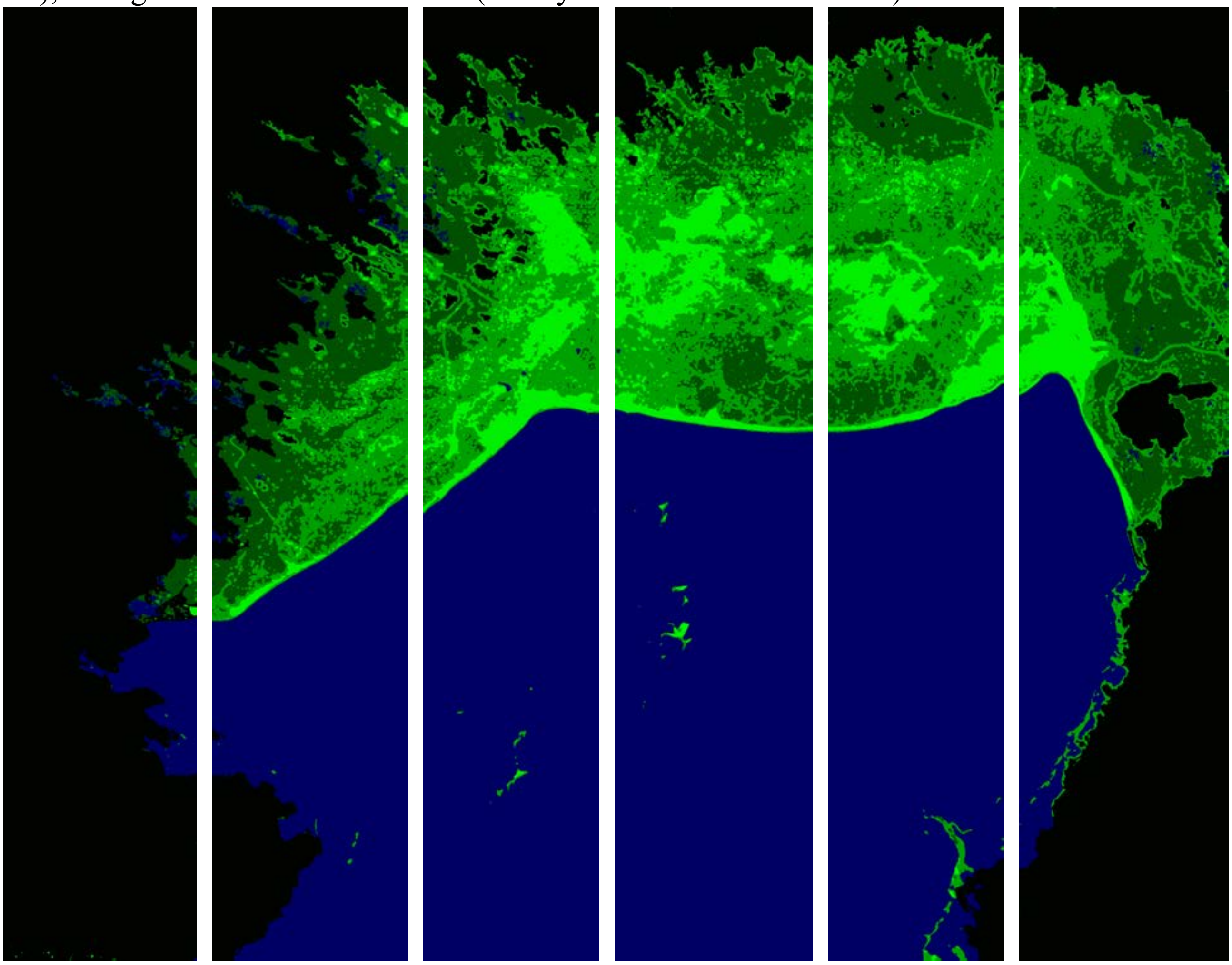

Figure 2. Classification into ice types open water, highly deformed pack ice, moderately deformed ice, moderately deformed ice, Feb, 27, 2014

For comparison, the readers may consider the ice chart of Feb, 27, 2014 of the official Swedish Ice Chart (SMHI) in Figure 3. The results coincide well with the official SMHI ice chart of the respective date. In particular, the areas of strong backscatter, which correspond to a high degree of deformation, are located in the same areas as in the SMHI ice chart. This is of particular importance for operational purposes, since these ice types are the most difficult to navigate.

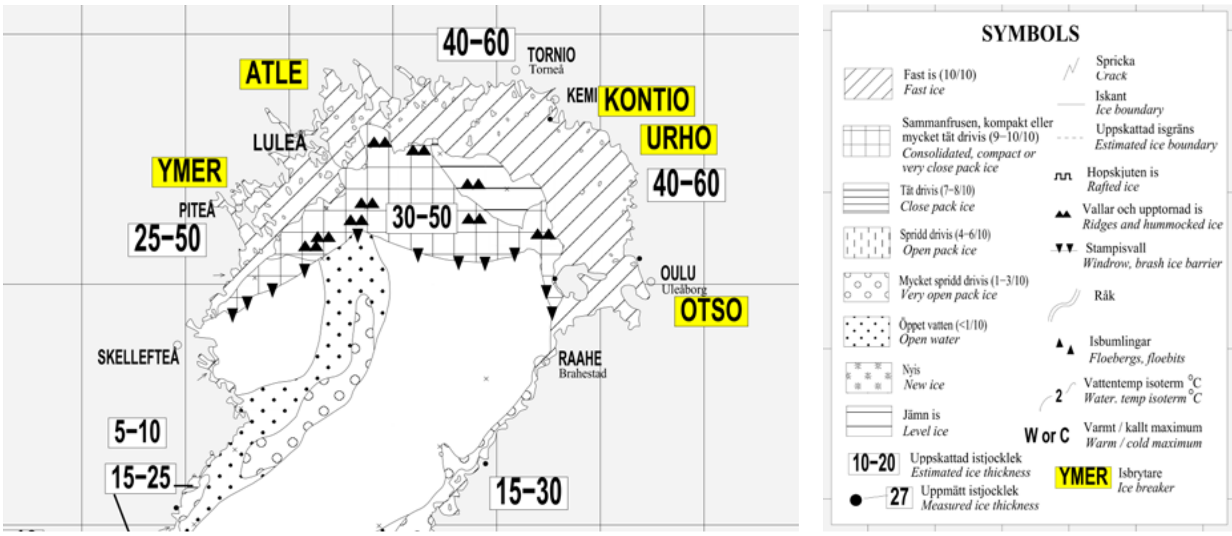

Figure 3. Official Ice Chart of the Swedish SMHI for Feb, 27, 2014

5. Conclusion

We successfully applied GLCM and LBP texture features to ScanSAR images of sea ice on one example of TerraSAR-X acquisitions of the Northern Baltic Sea. By visual analysis and by comparison with official ice charts we first identified the dominant ice classes in the image, then chose small patches of training data for the ice types from the image. These training data samples were then utilized for training an artificial neural network (FANN). The trained network executed the classification based on the extracted features. The result proves that our approach is a promising path towards an automated ice charting algorithm for near real time operational navigation assistance.

Acknowledgements

All TerraSAR-X images were obtained through DLR. The research underlying this work was conducted within the EMS Sea Ice research project funded by the German Ministry of Economy.

References

Bogdanov, A. , Sandven, S. , Johannessen, O. , Alexandrov, V. , and Bobylev, L., 2005. Multisensor Approach to Automated Classification of Sea Ice Image Data. IEEE Transactions on Geoscience and Remote Sensing, Vol. 43, No. 7, 1648-1664.

Clausi, D. 2010. Comparison and fusion of co-occurrence, Gabor and MRF texture features for classification of SAR sea-ice imagery. Atmosphere-Ocean, 39:3, 183-194.

Dierking, W., Pedersen, L., 2012. Monitoring sea ice using Envisat ASAR - A new era starting 10 years ago. IGARSS 2012, 1852-1855.

Hamidi, D., Lehner, S., König, T., and Pleskachevsky, A. 2011. On the Sea Ice Motion Estimation with Synthetic Aperture Radar. Proceedings of 4. TerraSAR-X Meeting (Vortrags-Nr. CAL0166), 1-10.

Haralick, R., Shanmugam, K. and Dinstein, I. 1973. Textural Features for Image Classification. IEEE Transactions on Systems, Man, and Cybernetics, Vol. 3, No. 6, 610-621.

Karvonen, J., Simila, M. and Makynen, M. 2004. Open Water Detection from Baltic Sea Ice SAR Imagery. Proc. IEEE International Geoscience and Remote Sensing Symposium (IGARSS'04), v. VII, 4382-4385.

Mäenpää, T. Ojala, M. Pietikäinen, and M. Soriano, 2000. Robust texture classification by subsets of local binary patterns. Proc. 15th International Conference on Pattern Recognition, Barcelona, Spain

Moen, M.-A.N., Doulgeris, A.P. Anfinsen, S.N. Renner, A.H.H. Hughes, N. Gerland S. and Eltoft, T., 2013. Comparison of automatic segmentation of full polarimetric SAR sea ice images with manually drawn ice charts. The Cryosphere, vol. 7, no. 6, 1693-1705.

Nissen, S., 2005. Neural Networks made simple. www.software20.org, 2/2005, 14-19.

Ojala, T. Pietikäinen, M. ,and Harwood, D., 1994. Performance evaluation of texture measures with classification based on Kullback discrimination of distributions. Proceedings of the 12th IAPR International Conference on Pattern Recognition (ICPR 1994), vol. 1, 582 - 585.

Soh, L.-K., C. Tsatsoulis, D. Gineris, and C. Bertoia, 2004. ARKTOS: An Intelligent System for Satellite Sea Ice Images. IEEE Transactions on Geoscience and Remote Sensing, 42(1), 229-248.

Soh, L.-K. and C. Tsatsoulis, 1999. Texture Analysis of SAR Sea Ice Imagery Using Gray Level Co-occurrence Matrices. IEEE Transactions on Geoscience and Remote Sensing, 37(2), 780-795.

Yu, Q., Moloney, C., Williams, F., 2002. SAR sea-ice texture classification using discrete wavelet transform based methods. GRSS, IGARSS 02, Vol 5 , 3041-3043.

Zakhvatkina, N., Alexandrov, V. ,Johannessen, O., Sandven, S. and Frolov, I., 2013. Classification of Sea Ice Types in ENVISAT Synthetic Aperture Radar Images. IEEE Transactions on Geoscience and remote Sensing, Vol. 51, No. 5, 2587-2600.